Missouri University of Science and Technology

Scholars' Mine

International Conferences on Recent Advances in Geotechnical Earthquake Engineering and Soil Dynamics

2010 - Fifth International Conference on Recent Advances in Geotechnical Earthquake Engineering and Soil Dynamics

29 May 2010, 8:00 am - 9:30 am

1D Dynamic Non-Linear Numerical Analysis of Earth Slopes: The Role of Soil Ductility and Time-Sensitiveness

Claudio Giulio di Prisco
Politecnico di Milano, Italy

Federico Pisanò
Politecnico di Milano, Italy

Follow this and additional works at: https://scholarsmine.mst.edu/icrageesd

 Part of the Geotechnical Engineering Commons

Recommended Citation

di Prisco, Claudio Giulio and Pisanò, Federico, "1D Dynamic Non-Linear Numerical Analysis of Earth Slopes: The Role of Soil Ductility and Time-Sensitiveness" (2010). *International Conferences on Recent Advances in Geotechnical Earthquake Engineering and Soil Dynamics*. 1.
https://scholarsmine.mst.edu/icrageesd/05icrageesd/session03b/1

This work is licensed under a Creative Commons Attribution-Noncommercial-No Derivative Works 4.0 License.

This Article - Conference proceedings is brought to you for free and open access by Scholars' Mine. It has been accepted for inclusion in International Conferences on Recent Advances in Geotechnical Earthquake Engineering and Soil Dynamics by an authorized administrator of Scholars' Mine. This work is protected by U. S. Copyright Law. Unauthorized use including reproduction for redistribution requires the permission of the copyright holder. For more information, please contact scholarsmine@mst.edu.


Fifth International Conference on
Recent Advances in Geotechnical Earthquake Engineering and Soil Dynamics
and Symposium in Honor of Professor I.M. Idriss
May 24-29, 2010 • San Diego, California

1D DYNAMIC NON-LINEAR NUMERICAL ANALYSIS OF EARTH SLOPES: THE ROLE OF SOIL DUCTILITY AND TIME-SENSITIVENESS

Claudio Giulio di Prisco
Politecnico di Milano
Milano, ITALY 20133

Federico Pisanò
Politecnico di Milano
Milano, ITALY 20133

ABSTRACT

The mechanical response of dry granular slopes subjected to dynamic perturbations is tackled from a theoretical/numerical viewpoint. A 1D geometrical/numerical scheme is adopted to analyze infinitely long strata: the dynamic activation of shallow translational failure mechanisms (as well as the displacement performance far from collapse) is analyzed by means of a self-made FEM code.

The soil mechanical behavior is described by means of a simplified viscoplastic one-dimensional constitutive model, capable of reproducing both ductile (hardening) and brittle (softening) mechanical responses. The dependence of numerical results on the soil "time-sensitiveness", as well as the differences between viscoplasticity and standard rate-independent plasticity, is discussed. For the case of impulse-like loads (Ricker wavelets), the influence of the ratio between the dominant wavelength and the stratum thickness on the overall deformation mechanism is commented. The response of the slope to a real accelerometric record is finally illustrated.

INTRODUCTION

Slope stability under dynamic/seismic actions is a very challenging topic in the field of earthquake geotechnical engineering. In the recent and less recent past the large losses in terms of both goods and human lives have put in evidence the crucial role could be played by the comprehension of the seismic response of natural earth slopes for the improvement of risk evaluation skills and mitigation techniques, at least as far as a local scale is concerned.

The most widespread approach for analyzing the dynamic performance of earth slopes is still based on the early Newmark's intuition, primarily conceived for earth dam and embankment applications (Newmark 1965). According to the Newmark approach, the slope is considered as a rigid-block sliding along a frictional interface, where all the irreversible displacement are supposed to be concentrated. In this approach several weaknesses can be envisaged: among these, the fundamental ones concern the assumption of rigid motion of the slope and the existence of a unique sliding surface. In order to extend the applicability of the rigid-block model, since 70s several strategies have been introduced in literature. For instance, among these the decoupled continuum/rigid block mixed method (Makdisi and Seed 1978) and the multi-block model (Kramer and Smith 1997) can be cited. An overview of several available simplified methods for seismic slope stability analysis is provided by Kramer (Kramer, 1997) and, more recently, by Bray (Bray, 2007).
Nevertheless, in the last decades the possibility of numerically simulating the dynamic mechanical response of slopes in 2D and 3D has been largely investigated and noticeable efforts have been done to improve the numerical treatment of coupled multiphase problems and the implementation of sophisticated constitutive relationships (Prevost *et al.* 1985, Zienkiewicz *et al.* 1999).

In this paper a trial for conjugating simplicity and a satisfactory description of essential problem aspects is proposed and, at the same time, some conceptual considerations about the problem of dynamic slope stability are stated. In particular, a simplified one-dimensional numerical model is employed to highlight the role played by the essential features of the soil mechanical behavior – like ductility and time-sensitiveness – in determining the dynamic performance of the slope. In this perspective, the suitability of a continuum approach is stressed once again, as, with respect to standard simplified methods, it allows for a better comprehension of physical phenomena.

NUMERICAL ALGORITHM AND CONSTITUTIVE MODEL

The boundary value problem analyzed hereafter concerns the propagation of shear waves across an inclined dry soil layer resting on a rigid bedrock. As the system is assumed to be infinite along the *x* direction (as well as along the out of plane one), the problem can be treated as one-dimensional, so that all the mechanical variables depend uniquely on the *z* coordinate: so the system geometry is fully determined once the stratum thickness *H* and its inclination α are assigned. A sketch of the problem is given in Fig. 1.

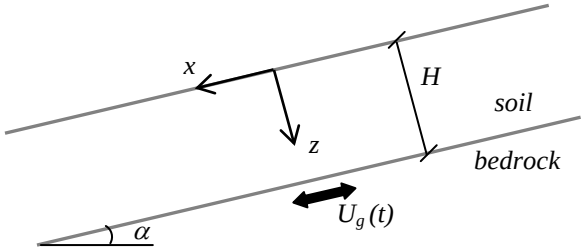

Fig. 1. Geometrical scheme of the analyzed boundary value problem.

Since the goal of this work is to study the dynamic performance of the stratum under shear disturbances, the problem has been further simplified by assuming, analogously to linear elasticity, the shear stress to be uniquely dependent on the corresponding shear strain. As a consequence the number of unknowns decreases abruptly, as the displacement, strain and stress fields are described by the following few components: the displacement $U(z)$ (along the *x* direction), the shear strain $\gamma(z)$, the stresses $\tau(z)$ (shear component) and $\sigma(z)$ (normal *z* component, statically determined as a function of both α and the soil unit weight). This assumption allows to obtain qualitatively reasonable results, although it implies two fundamental shortcomings: (i) as is well-known, all the normal components of the stress tensor influence the soil deviatoric response (in particular the inelastic one); (ii) a pure shear model cannot be extended to the case of a two-phase (solid-fluid) medium.

Numerical approximation

The set of differential equations governing the 1D motion of a continuum medium has been approximated through the standard Galerkin-Finite Element method (Zienkiewicz and Taylor, 2000), where the problem unknown is the nodal displacement vector $\boldsymbol{U}$. The bedrock is considered to be rigid and, as consequence, the $\boldsymbol{U}$ last component (at $z=H$) is imposed and set equal to the function $U_g(t)$ (Fig. 1), representing the input ground motion.

All the numerical results presented in the following have been obtained by performing the space discretization of the stratum by means of quadratic 1D finite elements, having three nodes and three quadrature points. The system has been integrated in time by employing the so-called *HHT/α-method* (Hilber *et al.*, 1977), which is a well-known improvement - unconditionally stable - of the standard Newmark algorithm (Newmark, 1959). Time marching requires at each step the solution of the non-linear global system through the Newton-Raphson algorithm. Moreover, a second iterative procedure is necessary for the discrete integration of the constitutive law at the Gauss point level. The solving scheme can be recognized implicit both globally and locally.

Viscoplastic constitutive shear model

The use of viscoplasticity is not yet so widespread for seismic applications, even though it is suitable for capturing the time-sensitiveness of the soil mechanical behavior. In order to stress the differences between viscoplasticity and the more popular Kelvin-Voigt viscoelastic model, in Fig. 2 a reological scheme of an elasto-viscoplastic model is sketched.

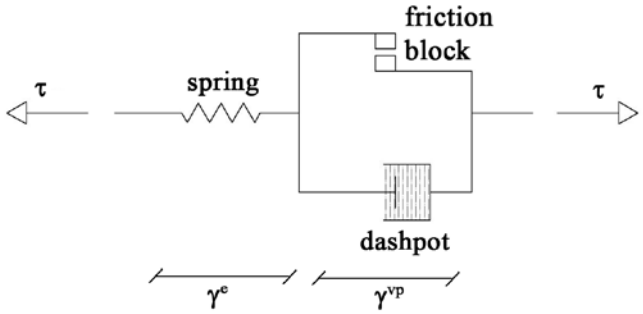

Fig. 2. Reological scheme of an elastoviscoplastic model.

Fig. 2 puts in evidence the following items:
(1) in viscoplasticity energy dissipation is associated to the development of inelastic strains, taking place (in case of perfect viscoplasticity) while exceeding the material strength (friction block in Fig. 2);
(2) similarly to a Maxwell viscoelastic model, once the inelastic behavior is triggered, the dashpot element (viscosity) and the spring (elasticity) work in series; the opposite is assumed in the parallel Kelvin-Voigt scheme.
(3)
As is well-known, this latter aspect plays an essential role in determining the soil damping properties and their dependence on the loading frequency. When the dashpot is put in series to the spring, the damping coefficient *D* – which is defined as usual – decreases with the frequency, in contradiction with what a Kelvin-Voigt constitutive law predicts. As far as this issue is concerned, in the last decades several authors (Shibuya *et al.* 1995, Santucci de Magistris *et al.* 1999, Meng 2003) have experimentally supported the idea that *D* is a decreasing function of frequency within a quite large frequency range, in particular when the cycle amplitudes are increased and the loading frequency reduced. In order to clarify this concept, in Fig. 3 a series of torsional shear

experimental test results are compared with the ideal trends would be simulated by employing elasto-hysteretic, Kelvin-Voigt viscoelastic and viscoplastic constitutive models. It is worth noting that standard elasto-plasticity merges in this figure the elasto-hysteretic curve. As is evident, the viscoelastic model seems to be appropriate only for high frequency values, whilst viscoplasticity fits satisfactorily the experimental data for low values.

Furthermore, the employment of elasto-viscoplasticity is further encouraged in case of slope stability problems, requiring as a crucial issue the prediction of irreversible displacements for evaluating the safety of the system (Newmark, 1965).

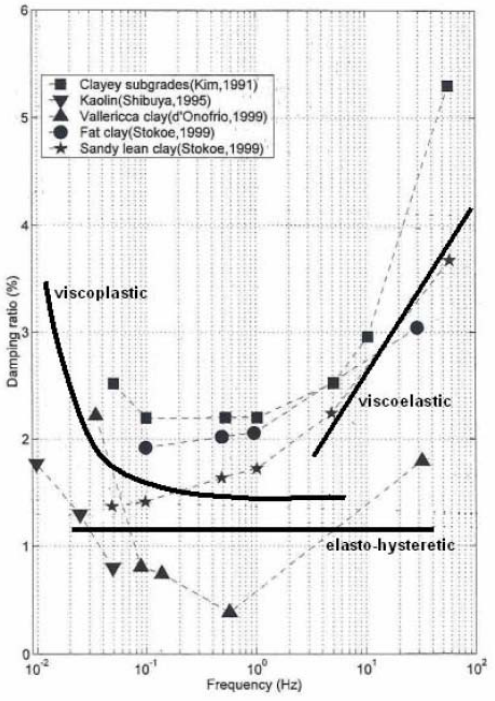

Fig. 3. Dependence of damping coefficient on loading frequency for different types of soil (from di Prisco et al., 2007).

As was mentioned above, the soil constitutive relationship is formulated as a τ-γ model. Its basic features are summarized here below:
(1) strains γ are small and they can be split into a linear-elastic part γ^e and an inelastic one γ^{vp}.
(2) the increment of γ^{vp} is evaluated according to the theory of standard viscoplasticity, by introducing a standard Perzyna viscous nucleus definition;
(3) the yield function f is defined in the τ-σ plane. Thanks to the constitutive relation employed and to the kind of dynamic perturbation imposed, the σ stress is constant in time;
(4) a isotropic strain-hardening constitutive relationship is introduced. The hardening variable φ (friction angle) defines the opening angle of the yield locus and it is assumed to evolve as a function of λ.

The constitutive equations can be written as it follows:

$$\begin{cases} a) \quad \tau = G\gamma^e = G\left(\gamma - \gamma^{vp}\right) \\ b) \quad f = |\tau| - \sigma \tan\phi(\lambda) \\ c) \quad \dot{\gamma}^{vp} = sign(\tau)\cdot\dot{\lambda} \\ d) \quad \dot{\lambda} = \eta\langle f/\sigma\rangle^m \end{cases} \tag{1}$$

where G is the elastic shear modulus, $\dot{\lambda}$ is the plastic multiplier, η ([s^{-1}], *fluidity parameter*) and m (dimensionless) are two viscoplastic parameters; dots stand for time derivative, whilst $\langle f/\sigma \rangle$ outputs 0 when the argument is negative and the argument itself when it is positive. The hardening rule, governing the local evolution of the tangent of φ, is expressed in a finite form as it follows:

$$\tan\phi = \begin{cases} \tan\phi_p + e^{-a\lambda}\left(\tan\phi_0 - \tan\phi_p\right) & \lambda \le \lambda_t \\ \tan\phi_r + e^{-b\lambda}\left(\tan\phi_t - \tan\phi_r\right) & \lambda > \lambda_t \end{cases} \tag{2}$$

where φ_0, φ_p and φ_r are constitutive parameters coinciding with the friction angle values at first yielding, at peak and at residual conditions respectively; the constitutive parameters a and b describe the evolution of $\tan\varphi$ versus λ, λ_t represents a threshold separating the hardening and the softening regime and φ_t is determined by enforcing the continuity of $\tan\varphi$ at $\lambda=\lambda_t$. For instance when λ_t is imposed equal to zero and $\varphi_p > \varphi_r$ the elasto-softening behavior can be reproduced (dashed line in Fig. 4). The hardening rule (2) can be set to reproduce several different behaviors, as for instance hardening/softening, purely hardening ($\varphi_0 < \varphi_p = \varphi_r$), elasto/softening ($\varphi_0 = \varphi_p > \varphi_r$) and also perfect viscoplasticity (no hardening, $\varphi_0 = \varphi_p = \varphi_r$). In Fig. 4 the hardening rules employed in the following are plotted.

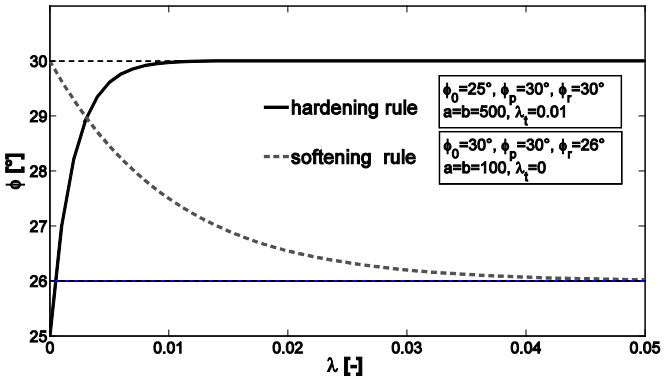

Fig. 4. φ-λ "hardening" and "softening" rules.

The proposed constitutive model is capable of capturing the effects of rate-dependency and ductile/brittle behaviors, but not of accurately reproducing the accumulation of irreversible strains during cyclic loading.

From a mathematical viewpoint, equations (1) allow to introduce the time-factor in the constitutive relationship by substituting the consistency rule with the definition of the viscous nucleus (eq. 1d). In this model inelastic strains do not develop instantaneously, since the shear strain rate is a function of the yield limit violation (eq. 1c). As is well-known, viscoplasticity can be considered as an intermediate step between elasticity and standard plasticity, as can be inferred from equation (1d). In order to clarify this concept in Fig. 5 the responses of a material point subjected to two different sinusoidal strain histories (same amplitudes but different frequencies) for different values of η are compared. When η=0 a purely elastic response is got, whilst by increasing η the standard rate-insensitive elasto-perfectly plastic response is progressively approached (in this case hardening has been neglected, $\varphi_0=\varphi_p=\varphi_r$).

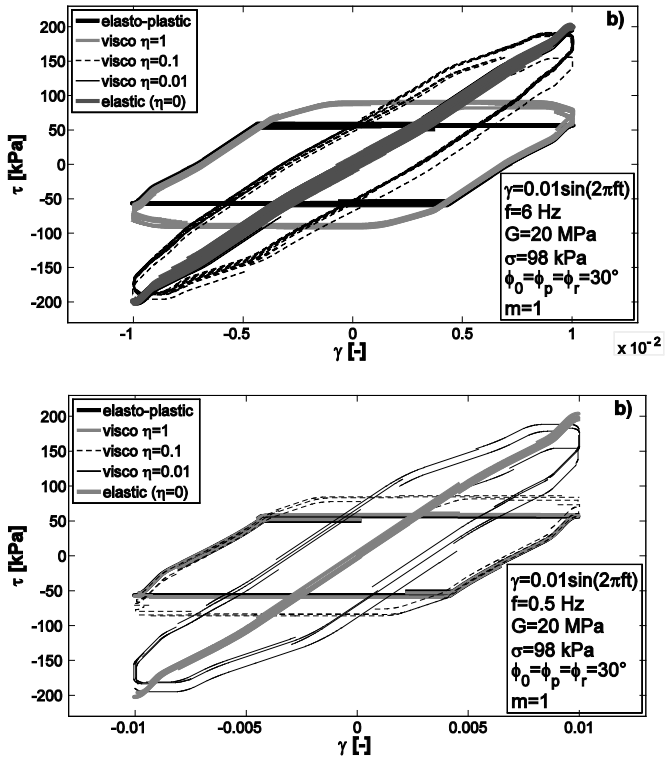

Fig. 5. Viscoplastic cyclic shear response for different η and loading frequency equal to (a) 6 Hz and (b) 0.5 Hz.

As previously mentioned, Fig. 5 clearly illustrates the dependence of the damping ratio D on both η and the loading frequency f.

NUMERICAL ANALYSES

In this section the results of several numerical analyses are presented. They concern the dynamic response of a soil stratum dynamically shaken by imposing a Ricker wavelet as an input ground motion. After an introduction about the usefulness of preliminary elastic analyses (§3.2), the influence on numerical results of the material rate-sensitiveness is discussed with reference to both the aforementioned ductile and brittle behaviors, also including in most cases a comparison with the time-independent (elasto-plastic) response (§3.3).

In the performed numerical analyses both the slope inclination α and the input motion have been kept fixed, and the influence of both the stratum thickness H (§3.3) and the elastic stiffness G (§3.4) (i.e. of the elastic shear wave velocity V_s too) is discussed.

In Table 1 the geometrical/mechanical parameters employed for non-linear analyses are summarized. Bold typeface symbols stand for kept constant parameters.

Table 1. Geometrical/Mechanical Properties.

GEOMETRY					
α [°]			**H [m]**		
25			10, 5, 2		
MATERIAL PARAMETERS					
Density/elastic					
δ [kg/m^3]		**G [MPa]**		**V_s [m/s]**	
2000		20,80,320		100, 200, 400	
Viscous					
η [s^{-1}]			**m [-]**		
1, 10, 50, ∞			**1**		
Plastic/Hardening					
φ_0 [°]	**φ_p [°]**	**φ_r [°]**	**a [-]**	**b [-]**	**λ_t [-]**
25	**30**	**30**	**500**	**500**	**0.01**
Plastic/Softening					
φ_0 [°]	**φ_p [°]**	**φ_r [°]**	**a [-]**	**b [-]**	**λ_t [-]**
30	**30**	**26**	**100**	**100**	**0**

(elasto-plastic analyses correspond with $\eta=\infty$).
Most results are presented in terms of inelastic strains, γ^{vp} (viscoplastic) and γ^{p} (plastic), and irreversible displacement U^{irr}, which is obtained by spatially integrating along z the unrecoverable strains:

$$U^{irr}(z,t)=\int_{z}^{H}\gamma^{vp/p}(z',t)\,dz' \qquad (3)$$

Input ground motion

All the numerical results presented in section 3 are obtained by imposing on the lower boundary the following displacement time history (Fig. 6):

$$U_g(t)=A\left[\beta(t-t_0)^2-f_p\right]\cdot\exp\left\{-\left[(\pi f_{\max})(t-t_0)\right]^2\right\} \qquad (4)$$

where t_0=0.25 s, f_{max}=6 Hz, f_p=0.01 Hz, β=7.106 m^{-3}, A=0.23022 m*s. The amplitude parameter A has been set in order to get a PGA=0.5 g.

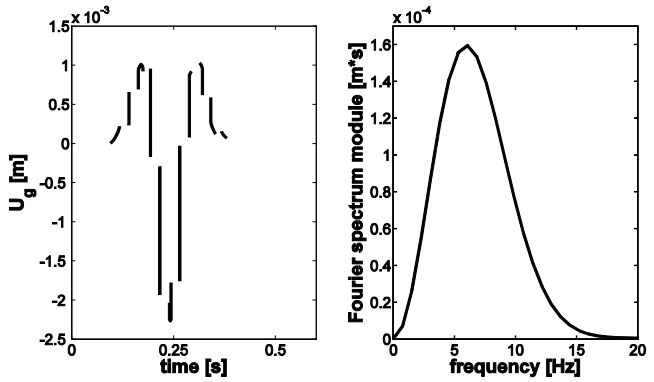

Fig. 6. Input ground motion/Ricker wavelet: (a) displacement time history and (b) Fourier spectrum.

As is well-known, the use of a Ricker wavelet allows to grasp some features of the system dynamic response as a function of geometrical and mechanical parameters. In truth slope movements triggered by impulse-like loading are also not infrequent, as in case of natural/artificial slopes in the vicinity of quarries.

Elastic prediction of the system mechanical response

The two standard approaches employed for interpreting the mechanical response of soil deposits consist in (i) performing 1D elastic numerical analyses to reproduce the wave propagation within the deformable medium, (ii) employing the previously mentioned Newmark method to quantify the irreversible displacements induced by seismic actions. Actually, preliminary elastic analyses can be useful for roughly understanding what kind of motion the slope undergoes (either synchronous or asynchronous) and for predicting the spatial distribution of the most stressed zones. This latter goal can be achieved, in case of frictional materials, by employing the material mobilized strength. This can be expressed, in a Mohr-Coulomb-like interpretation, by the mobilized friction angle φ_{mob}=arctan(τ/σ).

To graphically describe the spatial distribution of the most stress zones, the following procedure has been chosen:
(1) setting of the stratum thickness, calibration of the soil elastic properties and choice of the input ground motion with a reference peak amplitude;
(2) elasto-dynamic analysis;
(3) definition of the mobilized friction angle envelope, obtained at each depth z recording the φ_{mob} peak value during time.

In elasticity the dynamic stresses calculated are independent on the stratum inclination. Since in elasticity effects can be superimposed, the total stresses are obtained by adding to static stress distribution the dynamic one. Furthermore, the dynamic elastic solution is proportional to the imposed PGA: this implies a simple generalization of numerical results when in equation (4) solely parameter A is varied.

In Fig. 7 the elastic numerical results are plotted by taking into consideration the distribution of φ_{mob} peak values along the vertical axis. These results have been obtained by using the input signal in Fig. 6 and by considering different stratum thicknesses H (ranging from 20 to 1 m). The comparison is made meaningful by adopting a normalized depth z/H.

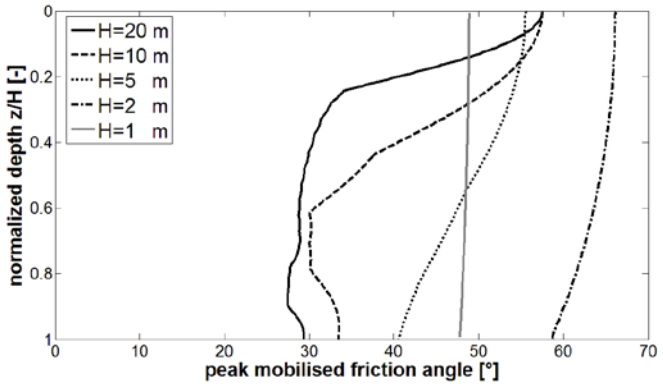

Fig. 7. Peak mobilized friction angles along depth for different H values (α=25°, δ=2000 kg/m^3, V_s=100 m/s).

The curves above highlight the transition through three different behaviors, associated to the H variation:
(1) for the largest thicknesses (20, 10 m) the most stressed zones are positioned at the top and bottom of the stratum. At the top the influence of the free surface condition is fundamental, as it implies a constructive interference of incident and reflected waves; at the bottom the soil/rock impendence ratio essentially determines the action severity, which is expected to decrease if more compliant bedrocks are considered;
(2) by gradually reducing H (5, 2 m), the aforementioned zones begin to interact, so that much more uniform distributions are found;
(3) If H is further decreased the distribution becomes almost uniform and the corresponding values progressively reduce: the limit value which is asymptotically reached coincides with the slope inclination α. Indeed, if the stratum becomes sufficiently thin, it moves simultaneously with the underlying bedrock, so that neither displacement gradients nor dynamic shear stresses are generated.
The mechanical responses briefly described here above are essentially due to the modification of both the Λ/H ratio (between the maximum wavelength propagating and the stratum height) and the mass of the soil deposit (Kramer and Smith 1997).

Obviously several ways for varying the Λ/H ratio can be conceived, as for instance the modification of the system elastic properties. In Fig. 8 the effect of a non-homogeneous distribution of the shear modulus G is illustrated, which is really known to increase in situ with the confining pressure (and so with the depth). The envelope in Fig. 7 concerning the 10 m-thick slope has been re-determined by assuming G to depend on z according to the following power-law:

$$G = G_0 \left(1+ z\right)^n \tag{5}$$

where G_0 has been set equal to 20 MPa (the previous constant value) and n is a dimensionless parameter governing the growth of G. When n=0 the distribution corresponding with G constant of Fig. 7 is obtained.

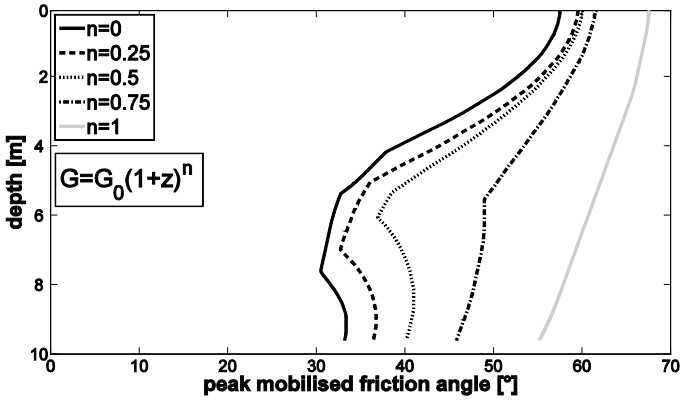

Fig. 8. Elastic peak mobilized friction angle for different depth-distributions of G (H=10 m, G_0=20 MPa→V_{s0}=100 m/s).

Such spatial soil stiffening plays qualitatively the role of a thickness shortening, as it has the effect of increasing the length of the propagated shear waves. The shape of the φ_{mob} envelope gradually modifies with the n value; for instance the curve obtained for n=1 (Fig. 8) looks very similar to that in Fig.7 corresponding to H=2 m and G constant along the depth.

Effects of soil non-linearity and rate-sensitiveness

Although elastic analyses can be usefully employed to understand how the system behaves under the imposed shaking, non-linear analyses are indispensible when the evaluation of irreversible displacements and/or the prediction of failure mechanism is requested. In this section the results of some parametric analyses are reported. These are aimed at clarifying the role played by the soil rate-sensitiveness and ductile or brittle behavior in determining – together with the geometrical parameters – the deformation of the slope.

The numerical results are shown by considering essentially three aspects: (i) the geometry, i.e. the stratum thickness H, (ii) the ductility of the soil mechanical response, i.e. the two different hardening rules in Fig. 4 are employed; (iii) the time-sensitiveness, i.e. the fluidity parameter η in eq. (1d) is varied. First of all the quantitative effect of η is illustrated (since m is kept constant). In Fig. 9 the U^{irr} time history at the top of the 10m-thick stratum is plotted: as a first step, no hardening/softening has been introduced, so that an elasto-perfectly viscoplastic model has been set (the parameter calibration is the same declared in Fig. 5).

As was expected, the η variation allows to recover the whole field ranging between elasticity (U^{irr} nil) and plasticity (which is the time-insensitive limit). The U^{irr} versus time curves calculated at the top put in evidence the progressive development of irreversible strains, associated to the wave propagation within the soil stratum. The numerical solutions appear to be very η-sensitive: it is evident that viscoplasticity is a tool to be handled with great care. The parameter η has to be calibrated on experimental test results, otherwise η could become just a parameter to be varied to adjust the numerical results.

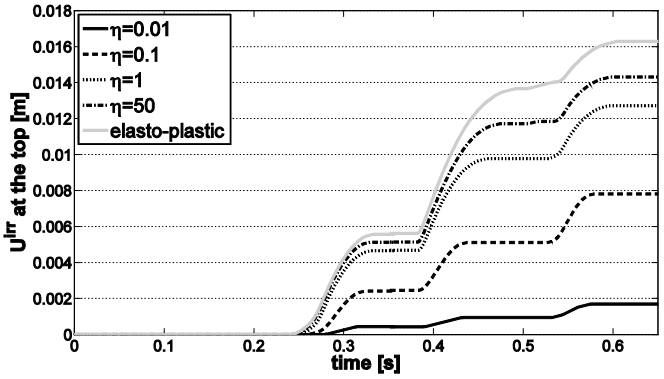

Fig. 9. Irreversible displacement vs time at the top of the soil stratum for different η values (α=25°, H=10 m, non-hardening model).

The effects of rate-sensitiveness are now considered with reference to the hardening model already described and calibrated in §2.2. In Fig. 10 the final spatial distributions (t=0.8 s) of both inelastic strains and displacements are reported (three different η values and three stratum thicknesses are considered). For the sake of completeness, the elasto-plastic case has also been analyzed.

The strain distributions are more spatially diffused for lower η values: such a smoothing effect can be considered in general a consequence of the delayed inelastic response. However, as far as the employed hardening model is concerned, beyond the threshold η=10 s^{-1} the difference between viscoplasticity and plasticity is almost negligible.

Qualitatively, H plays the same role already discussed with reference to elastic analyses. Passing from 10 m to 2 m, the γ^{vp} and γ^{p} distributions tend to become more uniform and their highest values to be shifted towards the lower zone of the

stratum. Nevertheless, in all the analyzed cases no localization occurs, although the elasto-plastic curve in Fig. 10e (H=2 m) shows a pronounced strain concentration at the soil/bedrock interface (but it is not sufficient for giving rise to a displacement discontinuity, Fig. 10f).

Then, the same analyses illustrated in Fig. 10 have been newly performed by employing the aforementioned softening model (see §2.2). The corresponding results are plotted in Fig. 11 (for the sake of brevity the γ^{vp} and γ^{p} distributions are reported only for the case H=10 m). In order to quantitatively compare the numerical results previously obtained with reference to the hardening ideal soil, as is illustrated in Fig. 4, the hardening and the softening rules are characterized by the same maximum φ value. The authors are aware that this assumption is not geotechnically meaningful, nevertheless this choice is quite convenient to put in evidence the material ductility importance in influencing the system mechanical response.

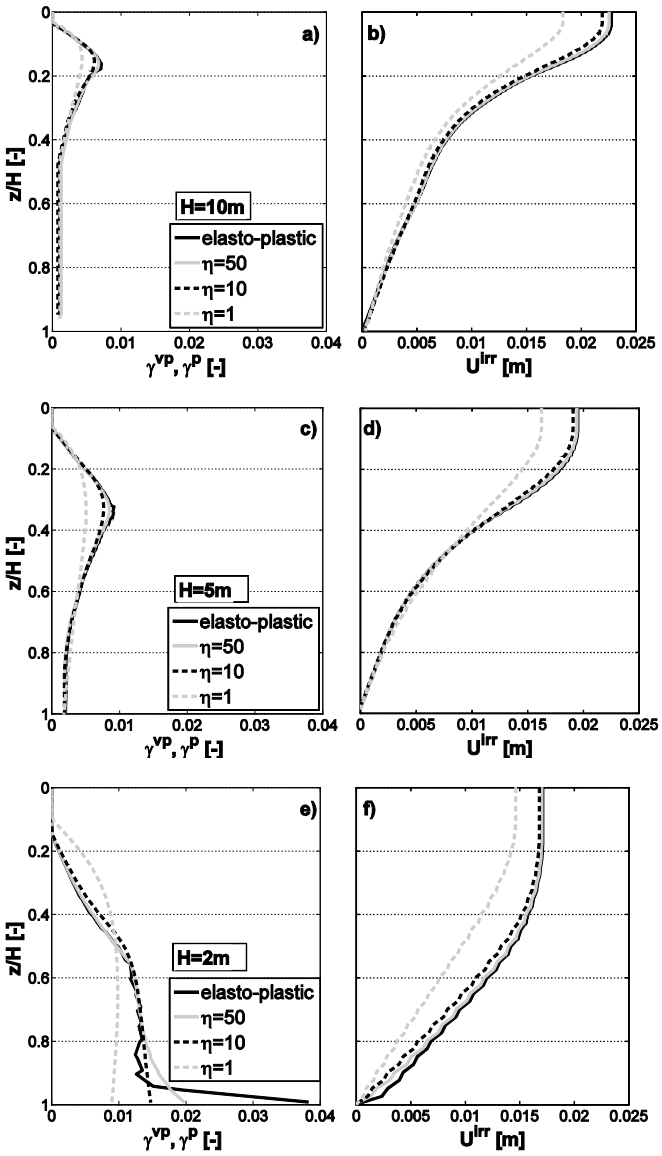

Fig. 10. Effect of rate-sensitiveness on the final spatial distribution of irreversible strain/displacement, for H equal to 10 m (a-b), 5 m (c-d) and 2 m (e-f) and α=25° (Hardening model).

By comparing the numerical results of Fig. 10-11 the following observations can be derived:

(1) in contrast with that observed in case of hardening, when a softening numerical analyses are performed localization can take place. The phenomenon is severely influenced by parameter η. While η being small enough, the curves obtained with the softening model are rather smooth; in contrast, when η=50 s^{-1} and even more for the elasto-plastic case, localization evidently occurs and a set of several shear bands can be observed for all the analyzed H values. In viscoplasticity, if a softening material is accounted for, the occurrence of localization is strictly connected to the soil time-sensitiveness: in other words, if the development of inelastic strains is time-

delayed enough, the formation of shear band is likely not to take place;
(2) even though localization appears, in none of the considered cases the Newmark single rigid block assumption seems to be fully applicable, but rather at least a multi-block model has to be employed. Unfortunately, predicting a priori the number and the position of the shear bands is not trivial at all, so that the necessity of full continuum non-linear dynamic analyses emerges.

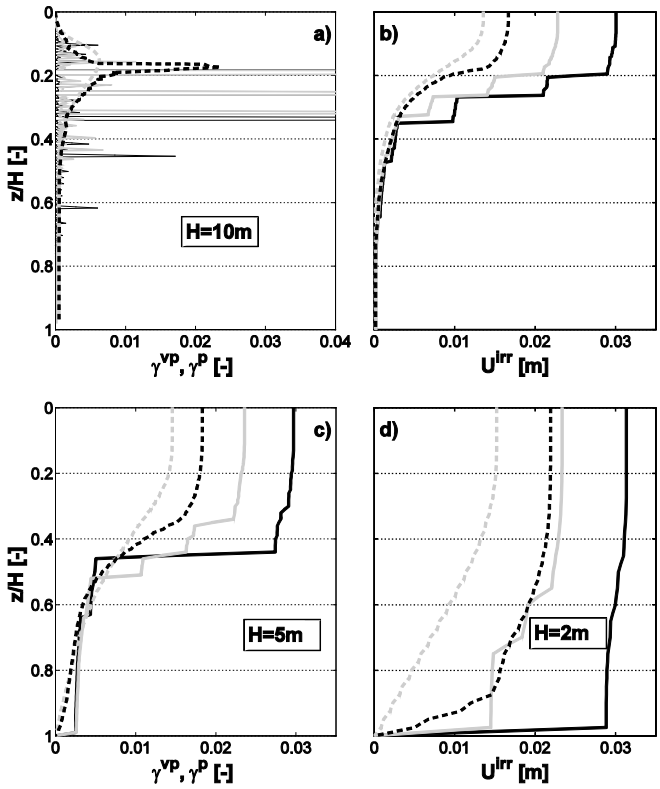

Fig. 11. Effect of rate-sensitiveness on the final spatial distribution of irreversible strain/displacement for H equal to 10 m (a-b), of 5 m (c) and 2 m (d) and α=25° (Softening model).

In all the examples discussed here above (also when localization is allowed to develop), the dynamic response can be defined to be stable, since the U^{irr} development stops when the inertial actions are exhausted. Indeed, the chosen residual friction angle (φ_r=26°) is larger than the slope inclination (α=25°). In Fig. 12, instead, it is exemplified the case in which $\varphi_r < \alpha$ and an unstable/collapsing response results.

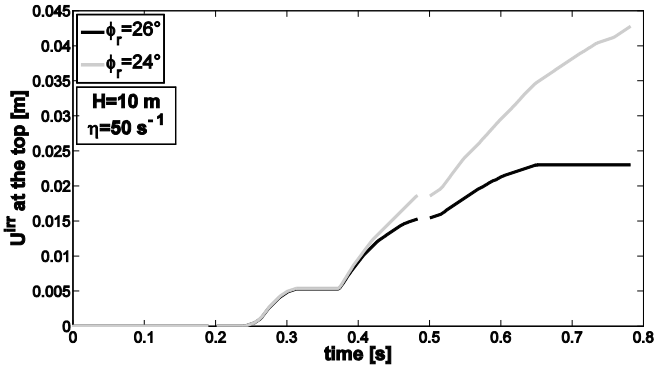

Fig. 12. Irreversible displacement vs time at the top of the soil stratum for two different residual friction angles in the softening model (α=25°, H=10 m, η=50 s^{-1}).

Since several parameters are involved in the definition of the Λ/H ratio, as stated above, the variation of the stratum thickness is not the unique way to modify the slope deformation. To stress this point, in Fig. 13 the results of some numerical analyses performed at varying values of the elastic shear wave velocity V_s are reported (Fig. 13a-b refer to the hardening case, Fig. 13c-d to the softening one). The qualitative effect of an increase in V_s seems to coincide in both cases: whilst in the former displacements remain continuous and the highest values of shear strains move progressively downward, in the latter is the position of shear bands moving downward.

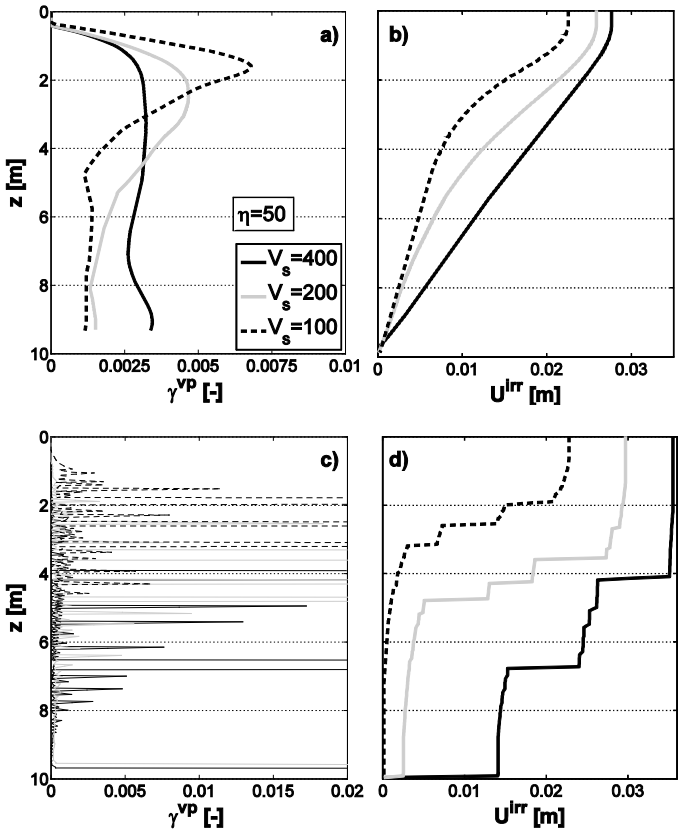

Fig. 13. Influence of the V_s value on the final spatial distribution of irreversible strain/displacement in the hardening (a-b) and softening cases (c-d) (α=25°, H=10 m, η=50 s^{-1}).

A similar trend could be obtained also by decreasing the dominant frequency of the input ground motion, since a decrease in the dominant frequency determines an increase in the maximum propagating wavelength (di Prisco *et al.* 2008).

Mesh-dependence of the numerical solution

As is well-known, when softening regimes are analyzed, the set of differential equations governing the standard elasto-plastic problem becomes ill-posed and the uniqueness of the solution is not ensured. By a numerical viewpoint this is detrimental, as it implies a "pathologic" dependence of the FE solution on the mesh size: by progressively refining the spatial discretization no convergence can be obtained and the shear band thickness tends to become infinitesimal. Instead, this variable should be finite and related to a material internal length. In contrast, several authors (Needleman 1988, Loret and Prevost 1990, Sluys 1992) showed the viscoplastic problem to always remain well-posed, giving rise to objective numerical solutions in both static and dynamic applications. This derives from the introduction of a material characteristic time, i.e. from the soil rate-sensitiveness (in the aforementioned model related to η). Indeed, since a viscoplastic medium requires a finite time to develop, the shear band thickness will be necessarily a function of both the wave frequency and the characteristic time.

In Fig. 14 these concepts are exemplified with reference to the analyses reported in Fig. 11d (H=2 m), but only relatively to the cases in which localization occurs (η=50 s^{-1} and elasto-plastic). To quantitatively describe the dependence of solution on the mesh-refinement, several FE results have been compared (for a number of elements ranging from 20 to 600). In Fig. 14a-b the plots of γ^{vp} and γ^{p} final distributions are magnified about the deepest shear band (each line marker corresponds to a single Gauss point). For the elasto-plastic case (Fig. 14a) the shear band width is always coincident with the decreasing FE size and the γ^{p} peak value tends to grow up indefinitely. On the contrary, the viscoplastic solutions (Fig. 14b) are characterized by the formation of a finite-sized shear band (about 3 cm) and by the convergence of the γ^{vp} values as well: also the coarser mesh (20 elements), which cannot capture the band thickness (elements are wider than 3 cm), provides a solution which seems to be just less accurate, not meaningless. In Fig. 14c-d results are shown in terms of U^{irr} distributions. As far as the elasto-plastic solutions are concerned, as a consequence of the band-narrowing, the main sliding mechanism at the bottom appears to be characterized by decreasing irreversible displacements.

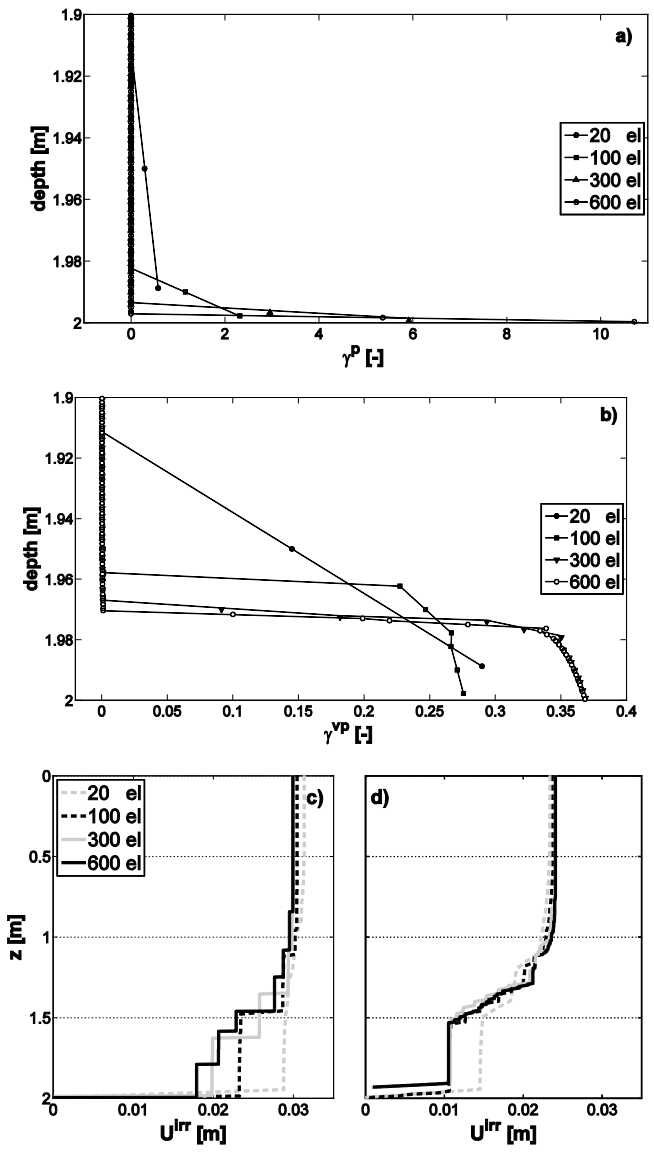

Fig. 14. Mesh-dependence of the numerical response for softening elasto-plastic and elasto-viscoplastic (η=50 s^{-1}) soils (α=25°, H=2 m). Localization of plastic (a) and viscoplastic (b) strains at the stratum bottom; comparison between the final U^{irr} profiles (c-d).

Nevertheless, viscoplasticity hides at least two shortcomings:
(1) despite some successful attempts (Sluys 1992), the a priori evaluation of the shear band width is not trivial at all, in particular when pronounced non-linearities in the constitutive relationship are introduced;
(2) since viscoplasticity tends to plasticity by inhibiting the rate-sensitiveness ($\eta \to \infty$), even the shear band thickness reduces gradually – even though the problem keeps its well-posedness – until unrealistic small values. In other words, viscous parameters are in general not sufficient at the same time to reproduce the time-dependence of the mechanical response and to describe the strain-localization.
(3)

Alternative strategies to deal with these problems consist in employing the so-called *high-order constitutive models* (*non-local* and *gradient* approaches, Pijaudier-Cabot and Bazant 1987, di Prisco *et al.* 2002), according to which the material characteristic length is introduced explicitly within the constitutive formulation. These approaches have been proven to be very effective for dealing with failure problems in brittle materials, but of course they involve a theoretical/computational effort larger than viscoplasticity.

THE CASE OF A REAL SEISMIC EXCITATION

In this section the remarks driven above are confirmed by considering an application in which a real seismic accelerometric record is imposed as input ground motion. In particular, a record from the recent M_L=5.8 L'Aquila earthquake (Italy, 2009-04-06, AQG station: R_{epi}=4.4 km, PGA=0.474 g) has been chosen (http://itaca.mi.ingv.it). From the whole record the most meaningful time-window of 20 seconds has been selected (Fig. 15a). In Fig. 15b the Fourier spectra (normalized with respect their peak amplitude value) of both input acceleration and displacement are reported. By comparing the Ricker wavelet displacement Fourier spectrum (Fig. 6b) with the corresponding one in Fig. 15b, it is evident that in the case of L'Aquila earthquake much lower frequencies are involved.

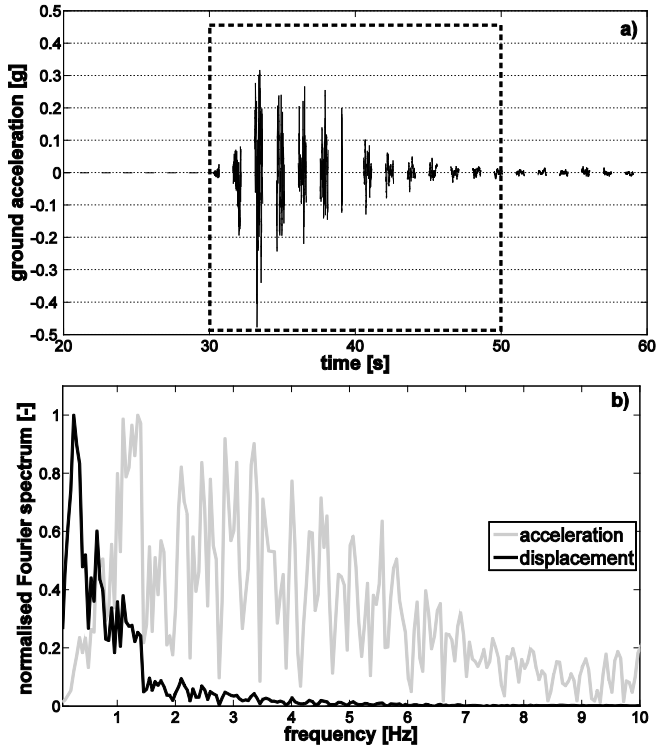

Fig. 15. L'Aquila earthquake: (a) an accelerometric record and (b) normalized Fourier spectrum of the recorded acceleration and of the time-integrated displacement.

The numerical results, concerning a 10 m-thick stratum, are obtained by imposing η=50 s^{-1} and by employing both the hardening and the softening versions of the aforementioned constitutive model.
In Fig. 16a both the simulated U^{irr} time histories at the top of the stratum are plotted. In Fig. 16b the final U^{irr} spatial distributions are compared. While in the hardening case the displacement field is everywhere continuous, in the softening one the soil brittleness together with a sufficiently high rate-sensitiveness gives rise again to the formation of several shear bands along the whole depth (as the involvement of low frequencies is expected to determine).

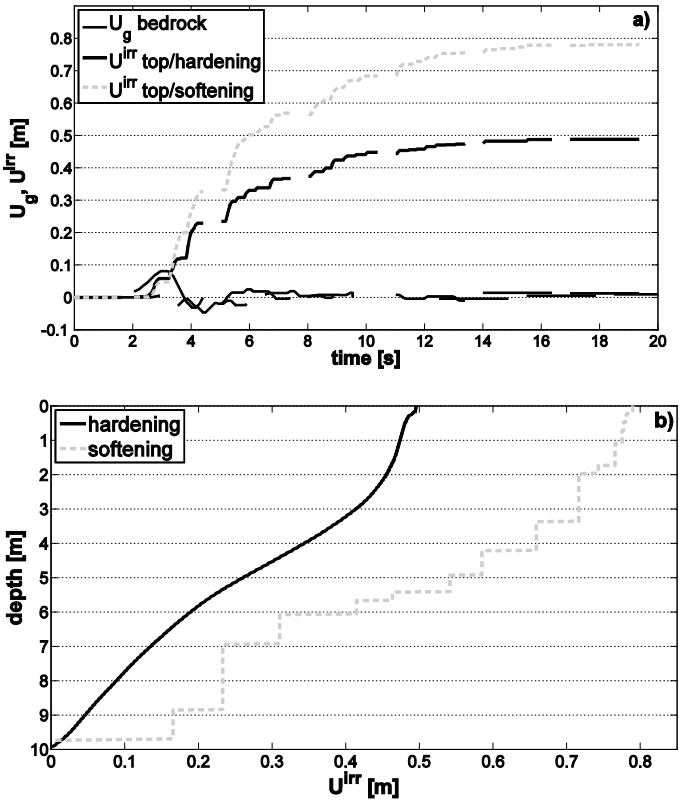

Fig. 16. Simulation of the viscoplastic slope response to the L'Aquila earthquake for the hardening and softening models (α=25°, H=10 m, η=50 s^{-1}): comparison between (a) the U^{irr} time histories of the top and (b) the U^{irr} final spatial distributions.

Under a qualitative viewpoint, the results obtained for the impulsive solicitation do not look so different from those corresponding to a real seismic input. However, as a consequence of the input complexity, in this latter case much larger irreversible displacements are predicted.

Finally, even if the growth of unrecoverable displacements is not unlimited and thus a proper slope collapse cannot be individualized, their accumulation can become excessive for any serviceability requirement.

CONCLUDING REMARKS

In this paper several aspects about the dynamic performance of earth slopes have been remarked. Under the simplifying assumption of a infinitely long slope, a 1D finite element code has been developed and employed to simulate the shear wave propagation within the system, caused by a prescribed ground motion of the underlying bedrock. The propagation of shear and volumetric disturbances have been supposed to be uncoupled also in the non-linear field. A 1D constitutive model has been adopted, formulated by providing the relationship between the shear stress and the associated shear strain component. The key-point of the constitutive formulation lies on the assumption of rate-dependency of the inelastic soil mechanical response, translated into the use of an elasto-viscoplastic model: in particular two distinct setting of the same model – hardening the former and softening the latter – have been compared, so that the differences between the dynamic response of ductile and brittle systems have been illustrated.

A special attention has been paid to the analysis of the deformation-mechanisms induced by input motions. Useful information to judge the suitability of simplified approaches has been derived. The main features of the slope deformation have been parametrically discussed by varying the stratum thickness, the soil elastic stiffness and the fluidity parameter. This last quantifies the "reactive" of the material in generating irreversible strains (comparisons with the rate-insensitive elasto-plastic case have been performed, too).

From the obtained numerical results the following conclusions can be inferred:
(1) the slope deformation depends essentially on the Λ/H ratio between the maximum propagating wavelength and the stratum height. By increasing this ratio, the inelastic strains suffered by the slope pass from a concentrated distribution in the upper zone of the deposit to a gradual smoothing of their spatial distribution (with a growing involvement of the lower zone). Before running non-linear analyses, several qualitative information about this issue have been derived from the results of elastic stress analyses;
(2) the introduction of soil viscosity has an important quantitative effect, since, by varying the fluidity parameter from zero to the infinity, the mechanical response passes from elastic to elasto-plastic. For this reason the calibration of viscous properties should be quite accurate. In general, the lowering of the viscous parameter entails a growing spatial diffusion of the viscoplastic strains and a reduction in their peak values;
(3) when a purely hardening soil behavior is assumed, the possibility of shear band generation is, in the framework of a τ-γ model, prevented. Nevertheless, even if the slope does not properly "fail", the evaluation of irreversible displacements is crucial, because a "loss of serviceability" of the system can occur. In contrast, when a brittle/softening behavior is taken into account, strain localization can really occur, as long as the inelastic response of the material is sufficiently fast (i.e. the

fluidity parameter is large enough). In such cases the employment of a viscoplastic model is not only an enhancement of standard elasto-plasticity, but also a simple way to keep the problem well-posedness and to get objective solutions. This due to the material "characteristic length" implicitly embedded in the viscoplastic formulation, as a consequence of rate-sensitiveness;
(4) Also in the cases in which localized failure takes place, the simulation of the real wave propagation phenomenon seems hard to be substituted by other simplified approaches (rigid-block models), since the number and the position of the shear bands are not a priori predictable.

Finally, an attempt to extend the aforementioned conclusions to more practical applications has been done by considering the case of a real sesmic input ground motion.

REFERENCES

Bray, J. D. [2007]. "Simplified seismic slope displacement procedures", in *Earthquake Geotechnical Engineering*, (K.D. Pitilakis, ed.), Springer, Dordrecht, Netherlands, pp. 327-353.

di Prisco, C., Imposimato, S. and Aifantis, E.C. [2002]. "A visco-plastic constitutive model for granular soils modified according to non-local and gradient approaches", Int. J. Num. Anal. Meth. Geomech., No. 26, pp. 121-138.

di Prisco, C., Stupazzini, M. and Zambelli, C. [2007]. "Nonlinear SEM numerical analyses of dry dense sand specimens under rapid and dynamic loading", Int. J. Num. Anal. Meth. Geomech., No. 31, pp. 757-788.

di Prisco, C., Pisanò, F., Imposimato, S. and Zambelli, C. [2008], "Dynamic Mechanical Response of Inclined Dry Granular Sand Strata", *Proc. Seismic Engineering. Conf. MERCEA08*, Reggio Calabria, ITALY, Vol. II, pp. 1179-1183.

Hilber, H., Hughes, T.J.R. and Taylor, R.L. [1977]. "Improved numerical dissipation for the time integration algorithms in structural dynamics", Earthquake. Eng. Struct. Dyn., No. 5, pp. 67-94.

Kramer, S.L. [1996]. "*Geotechnical Earthquake Engineering*", Prentice Hall, New Jersey.

Kramer, S.L. and Smith, M.W. [1997]. "Modified Newmark model for seismic displacements of compliant slopes", ASCE J. Geotech. Geoenv. Eng., No. 123, pp. 635-644.

Loret, B. and Prevost, J.H [1990]. "Dynamic strain localization in elasto-(visco-) plastic solids. Part 1. General formulation and one-dimensional examples", Comput. Meth. Appl. Mech. Engrg., No. 83, pp. 247-273.

Makdisi, F. and Seed, H. [1978]. "Simplified procedure for estimating dam and embankment earthquake induced deformations", ASCE J. Geot. Eng., No. 104, pp. 849-867.

Meng, J. [2003]. "*Simultaneous determination of shear modulus and damping ratio*", PhD thesis, Georgia Institute of Technology, Atlanta, Usa.

Needleman, A. [1988]. "Material rate dependence and mesh sensitivity in localization problems", Comput. Methods in Appl. Mech. Engrg., No. 67, pp. 69-85.

Newmark, N. [1959]. "A method of computation for structural dynamics", J. Eng. Mech. Div., No. 85, pp. 67-94.

Newmark, N. [1965]. "Effect of earthquake on dams and embankments", Geotéchnique, No. 15, pp. 139-160.

Pijaudier-Cabot, G. and Bazant, Z.P. [1987]. "Non-local damage theory", ASCE J. Engng. Mech.; No. 113, pp. 1512–1533.

Prevost, J.H., Abdel-Ghaffar, A.M. and Lacy, S.J. [1985]. "Nonlinear dynamic analysis of earth dams: a comparative study", ASCE J. Geot. Eng., No. 111, pp. 882-897.

Santucci de Magistris, F., Koseki, J., Amaya, M., Hamaya, S., Sato, T., Tatsuoka, F. [1999]. "A triaxial testing system to evaluate stress-strain behaviour of soils for wide range of strain and strain rate", ASTM Geot. Testing J., No. 22, pp. 44-60.

Shibuya, S., Mitachi, T., Fukuda, F., Degoshi, T. [1995]. "Strain rate effects on shear modulus and damping of normally consolidated clay", ASTM Geot. Testing J., No. 18, pp. 365-375.

Sluys, L.J. [1992]. "*Wave propagation, localisation and dispersion in softening solids*". PhD Thesis, Delft University of Technology, The Netherlands.

Zienkiewicz, O.C., Chan, A.H.C., Pastor, M., Schrefler, B.A. and Shiomi, T. [1999]. "*Computational Geomechanics with special reference to Earthquake Engineering*", John Wiley & Sons, Chichester, England.

Zienkiewicz, O.C. and Taylor, R.L [2000]. "*The Finite Element Method*" (5^{th} edition), Butterworth-Heinemann, Oxford, England.